J|A|C|S
ARTICLES
Published on Web 09/01/2006

# One-Electron Reduction of Kinetically Stabilized Dipnictenes: Synthesis of Dipnictene Anion Radicals

Takahiro Sasamori,[†] Eiko Mieda,[†] Noriyoshi Nagahora,[†] Kazunobu Sato,[‡] Daisuke Shiomi,[‡] Takeji Takui,[‡] Yoshinobu Hosoi,[§] Yukio Furukawa,[§] Nozomi Takagi,[||] Shigeru Nagase,[||] and Norihiro Tokitoh*,[†]

*Contribution from the Institute for Chemical Research, Kyoto University, Gokasho, Uji, Kyoto 611-0011, Japan, Graduate School of Science, Osaka City University, 3-3-138 Sugimoto, Sumiyoshi-ku, Osaka 558-8585, Japan, Department of Chemistry, School of Science and Engineering, Waseda University, 3-4-1 Okubo, Shinjuku-ku, Tokyo 169-8555, Japan, and Department of Theoretical Molecular Science, Institute for Molecular Science, Myodaiji, Okazaki 444-8585, Japan*

Received June 20, 2006; E-mail: tokitoh@boc.kuicr.kyoto-u.ac.jp

***Abstract:*** The redox behavior of kinetically stabilized dipnictenes, BbtE═EBbt [E = P, Sb, Bi; Bbt = 2,6-bis[bis(trimethylsilyl)methyl]-4-[tris(trimethylsilyl)methyl]phenyl], was systematically disclosed using cyclic voltammetry and theoretical calculations. It was found that they showed reversible one-electron redox couples in the reduction region. The anion radical species of the Bbt-substituted diphosphene and distibene were successfully synthesized by the reduction of the corresponding neutral dipnictenes (BbtP═PBbt and BbtSb═SbBbt). Their structures were reasonably characterized by ESR, UV−vis, and Raman spectroscopy, and the distibene anion radical was structurally characterized by X-ray crystallographic analysis.

## Introduction

The chemistry of low-coordinated compounds of heavier group 15 elements has been one of the most attractive areas since the first isolation of a diphosphene (Mes*P═PMes*, Mes* = 2,4,6-tri-*tert*-butylphenyl) by taking advantage of kinetic stabilization.[1] Up to now, several examples of diphosphenes (RP═PR)[2] and diarsenes (RAs═AsR)[2−4] were synthesized as stable compounds utilizing kinetic stabilization, and their structures and properties were revealed from various standpoints. It is generally accepted that the LUMO of a diphosphene is mainly the P═P $\pi^*$ molecular orbital,[2,5] where the $\pi^*$ orbital level is lower than that of the N═N double bond due to the smaller overlap of 3p orbitals of P atoms than that of 2p orbitals of N atoms.[5g] Indeed, it has been revealed that the P═P double bonds are easily reduced to afford the corresponding anion radical species[6] owing to the weaker $\pi$ bonds and the low lying $\pi^*$ orbital as compared with those of an N═N double bond. Such unique features of the $\pi$ electron systems of heavier main group elements are important and interesting from the viewpoints of not only fundamental chemistry but also material chemistry.[6,7] However, isolation and structural characterization of the anion radicals of heavier dipnictenes have not been reported probably due to their extremely high reactivity and/or instability, though there are a number of reports on the generation and ESR observation of anion radical species of diphosphenes,[6,8a] diarsenes,[8a] and phosphaarsenes.[8]

Since we have succeeded in the synthesis of the first stable distibene (**2a**)[9,10] and dibismuthene (**3a**)[9,11] by invoking an efficient steric protection group, 2,4,6-[$CH(SiMe_3)_2$]$_3C_6H_2$

[†] Kyoto University.
[‡] Osaka City University.
[§] Waseda University.
[||] Institute for Molecular Science.

(1) Yoshifuji, M.; Shima, I.; Inamoto, N.; Hirotsu, K.; Higuchi, T. *J. Am. Chem. Soc.* **1981**, *103*, 4587.
(2) For reviews, see: (a) Weber, L. *Chem. Rev.* **1992**, *92*, 1839. (b) Cowley, A. H.; Kilduff, J. E.; Lasch, J. G.; Mehrotra, S. K.; Norman, N. C.; Pakulski, M.; Whittlesey, B. R.; Atwood, J. L.; Hunter, W. E. *Inorg. Chem.* **1984**, *23*, 2582. (c) Tokitoh, N. *J. Organomet. Chem.* **2000**, *611*, 217.
(3) (a) Cowley, A. H.; Lasch, J. G.; Norman, N. C.; Pakulski, M. *J. Am. Chem. Soc.* **1983**, *105*, 5506. (b) Couret, C.; Escudié, J.; Madaule, Y.; Ranaivonjatovo, H.; Wolf, J.-G. *Tetrahedron Lett.* **1983**, *24*, 2769. (c) Cowley, A. H.; Norman, N. C.; Pakulski, M. *J. Chem. Soc., Dalton Trans.* **1985**, 383. (d) Smith, R. C.; Gantzel, P.; Rheingold, A. L.; Protasiewicz, J. D. *Organometallics* **2004**, *23*, 5124.
(4) Twamley, B.; Sofield, C. D.; Olmstead, M. M.; Power, P. P. *J. Am. Chem. Soc.* **1999**, *121*, 3357.
(5) A number of theoretical calculations (ab initio and semiempirical) for diphosphenes have been reported. For examples, see: (a) Yoshifuji, M.; Shibayama, K.; Inamoto, N. *J. Am. Chem. Soc.* **1983**, *105*, 2495. (b) Yoshifuji, M.; Hashida, T.; Inamoto, N.; Hirotsu, K.; Horiuchi, T.; Higuchi, T.; Ito, K.; Nagase, S. *Angew. Chem., Int. Ed. Engl.* **1985**, *24*, 211. (c) Gleiter, R.; Friedrich, G.; Yoshifuji, M.; Shibayama, K.; Inamoto, N. *Chem. Lett.* **1984**, *1984*, 313. (d) Cotton, F. A.; Cowley, A. H.; Feng, X. *J. Am. Chem. Soc.* **1998**, *120*, 1795. (e) Nagase, S.; Suzuki, S.; Kurakake, T. *J. Chem. Soc., Chem. Commun.* **1990**, 1724. (f) Allen, T. L.; Scheiner, A. C.; Yamaguchi, Y.; Schaefer, H. F. *J. Am. Chem. Soc.* **1986**, *108*, 7579. (g) Ito, K.; Nagase, S. *Chem. Phys. Lett.* **1986**, *126*, 531.
(6) (a) Çetinkaya, B.; Hudson, A.; Lappert, M. F.; Goldwhite, H. *J. Chem. Soc., Chem. Commun.* **1982**, 609. (b) Çetinkaya, B.; Hitchcock, P. B.; Lappert, M. F.; Thorne, A. J.; Goldwhite, H. *J. Chem. Soc., Chem. Commun.* **1982**, 691. (c) Culcasi, M.; Gronchi, G.; Escudie, J.; Couret, C.; Pujol, L.; Tordo, P. *J. Am. Chem. Soc.* **1986**, *108*, 3130. (d) Shah, S.; Burdette, S. C.; Swavey, S.; Urbach, F. L.; Protasiewicz, J. D. *Organometallics* **1997**, *16*, 3395. (e) Allen, T. L.; Scheiner, A. C.; Schaefer, H. F. *J. Phys. Chem.* **1990**, *94*, 7780. (f) Binder, H.; Riegel, B.; Heckmann, G.; Moscherosch, M.; Kaim, W.; vonSchnering, H. G.; Honle, W.; Flad, H. J.; Savin, A. *Inorg. Chem.* **1996**, *35*, 2119. (g) Geier, J.; Harmer, J.; Grützmacher, H. *Angew. Chem., Int. Ed.* **2004**, *43*, 4093.
(7) (a) Dutan, C.; Shah, S.; Smith, R. C.; Choua, S.; Berclaz, T.; Geoffroy, M.; Protasiewicz, J. D. *Inorg. Chem.* **2003**, *42*, 6241. (b) Nagahora, N.; Sasamori, T.; Takeda, N.; Tokitoh, N. *Chem.−Eur. J.* **2004**, *10*, 6146. (c) Nagahora, N.; Sasamori, T.; Tokitoh, N. *Chem. Lett.* **2006**, *35*, 220. (d) Smith, R. C.; Protasiewicz, J. D. *J. Am. Chem. Soc.* **2004**, *126*, 2268.

 **10.1021/ja064062m CCC: $33.50** 

***Scheme 1***

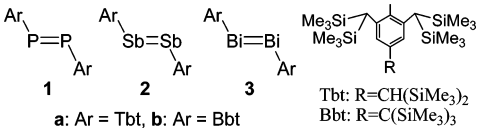


(denoted as Tbt), the doubly bonded systems of the heavier group 15 elements (dipnictenes) are no longer imaginary species even in the case of bismuth, the heaviest element among those that have a stable isotope. However, we could not sufficiently elucidate their reactivities of these new dipnictenes in solution because of their extremely low solubility in common organic solvents. Later on, Power and co-workers also synthesized another type of stable dipnictenes (diphosphenes, diarsenes, distibenes, and dibismuthenes) substituted by bulky 2,6-$Ar_2C_6H_3$ groups (Ar = mesityl or 2,4,6-triisopropylphenyl).[4] We have developed another bulky aromatic substituent, the 2,6-bis[bis(trimethylsilyl)methyl]-4-[tris(trimethylsilyl)methyl]phenyl (denoted as Bbt) group, and applied the Bbt group to the kinetic stabilization of dipnictenes. Finally, we have obtained the stable dipnictenes, **1a**,**b**,[12] **2a**,**b**,[9] and **3a**,**b**,[9] utilizing the Tbt and Bbt groups (Scheme 1) and reported their unique structures and properties. In contrast to the Tbt-substituted dipnictenes, **1a**, **2a**, and **3b**, the Bbt-substituted dipnictenes possess sufficient solubility in organic solvents to investigate their physical and chemical properties. Recently, we have preliminarily reported the systematic studies on the electrochemical redox behavior of **1b**, **2b**, and **3b** based on cyclic voltammetry,[13] showing that **1b**, **2b**, and **3b** display reversible one-electron reduction couples and that the distibene system has the lowest reduction potential among the corresponding dipnictenes. We present here the details of the electrochemical properties of Bbt-substituted diphosphene (**1b**), distibene (**2b**), and dibismuthene (**3b**) using cyclic voltammetry together with theoretical calculations. Furthermore, the anion radical species of diphosphene **1b** and distibene **2b** were synthesized as stable crystalline compounds $[Li^+(dme)_3][Bbt_2E_2^{\bullet-}]$ (E = P, Sb) by the chemical reactions of **1b** and **2b** using lithium metal as a reducing agent. The properties of $\mathbf{1b}^{\bullet-}$ and $\mathbf{2b}^{\bullet-}$ were disclosed by ESR, UV−vis, and Raman spectroscopy, and the distibene anion radical ($\mathbf{2b}^{\bullet-}$) was structurally characterized by X-ray crystallographic analysis.

## Results and Discussions

**Cyclic Voltammograms of Diphosphene 1b, Distibene 2b, and Dibismuthene 3b.** Kinetically stabilized diphosphene **1b**, distibene **2b**, and dibismuthene **3b** can be easily prepared via reductive coupling reactions of the corresponding dihalide ($BbtPCl_2$, $BbtSbBr_2$, $BbtBiBr_2$) using Mg metal.[9] Cyclic voltammetry should be a proper method for the purpose of elucidation of electrochemical properties. In Figure 1 the cyclic voltammograms for the oxidation (in $CH_2Cl_2$) and reduction (in THF) regions, respectively, are shown. In the oxidation region (Figure 1a), irreversible oxidation waves were observed for **1b**, **2b**, and **3b** around $E_{pa}$ = +1.01, +1.02, and +0.74 V vs $Ag/Ag^+$, respectively, suggesting that the corresponding radical cations and/or dications of **1b**, **2b**, and **3b** are unstable under these conditions. Theoretical calculations cannot give definite information for the oxidation state because details of the HOMO of RE═ER (R = H, Me, Ph, Mes; E = P, As, Sb, Bi) are very ambiguous and the energy levels of their $\pi$ orbitals are close to those of the $n_+$ orbital (in phase integration of lone pairs).[2,4,14,15] Therefore, it is somewhat difficult to draw a conclusion concerning the oxidation state of the dipnictenes on the basis of the experimental results obtained here. On the other hand, one can see that **1b**, **2b**, and **3b** showed reversible one-electron redox couples in the reduction region, respectively (Figure 1b). It should be noted that distibene **2b** showed the lowest $E_{1/2}$ as the reduction potential among the three dipnictenes examined. The experimental results observed here indicate that a distibene system may undergo the facile one-electron reduction as compared with the other heavier dipnictenes.

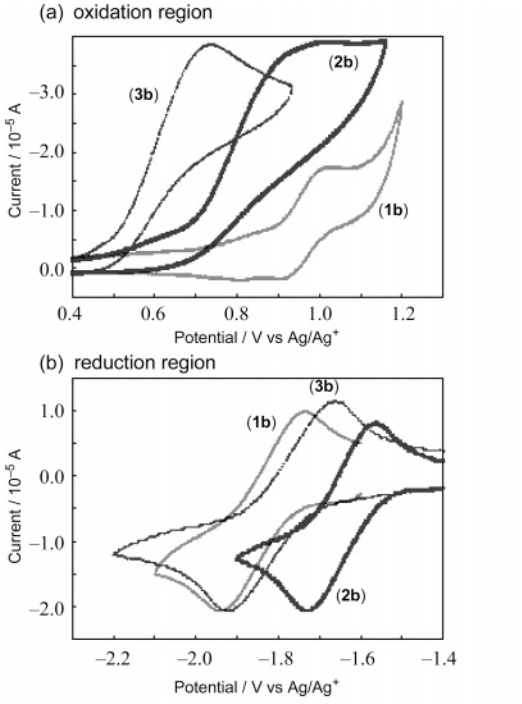


| | (a) | (b) | | |
|---|---|---|---|---|
| Redox Potential | $E_{pa}$ | $E_{pc}$ | $E_{pa}$ | $E_{1/2}$ |
| (**1b**)BbtP=PBbt | +1.011 | −1.94 | −1.74 | −1.84 |
| (**2b**)BbtSb=SbBbt | +1.021 | −1.73 | −1.56 | −1.65 |
| (**3b**)BbtBi=BiBbt | +0.735 | −1.92 | −1.66 | −1.79 |

***Figure 1.*** Cyclic voltammograms of BbtE═EBbt [E = P (**1b**), Sb (**2b**), Bi (**3b**)] (a) in $CH_2Cl_2$ with $Bu_4N^+BF_4^-$ (0.1 M) at −50 °C with a scan rate of 50 mV $s^{-1}$ and (b) in THF with $Bu_4N^+PF_6^-$ (0.1 M) at room temperature with a scan rate of 50 mV $s^{-1}$.

**DFT Calculations on the Reduction of Diphosphenes, Distibenes, and Dibismuthenes.** We performed DFT calcula-

(8) (a) Bard, A. J.; Cowley, A. H.; Kilduff, J. E.; Leland, J. K.; Norman, N. C.; Pakulski, M.; Heath, G. A. *J. Chem. Soc., Dalton Trans.* **1987**, 249. (b) Geoffroy, M.; Jouaiti, A.; Terron, G.; Cattanilorente, M.; Ellinger, Y. *J. Phys. Chem.* **1992**, *96*, 8241. (c) Tsuji, K.; Fujii, Y.; Sasaki, S.; Yoshifuji, M. *Chem. Lett.* **1997**, 855.
(9) Sasamori, T.; Arai, Y.; Takeda, N.; Okazaki, R.; Furukawa, Y.; Kimura, M.; Nagase, S.; Tokitoh, N. *Bull. Chem. Soc. Jpn.* **2002**, *75*, 661.
(10) (a) Tokitoh, N.; Arai, Y.; Sasamori, T.; Okazaki, R.; Nagase, S.; Uekusa, H.; Ohashi, Y. *J. Am. Chem. Soc.* **1998**, *120*, 433. (b) Tokitoh, N.; Sasamori, T.; Okazaki, R. *Chem. Lett.* **1998**, *27*, 725.
(11) Tokitoh, N.; Arai, Y.; Okazaki, R.; Nagase, S. *Science* **1997**, *277*, 78.
(12) Sasamori, T.; Takeda, N.; Tokitoh, N. *J. Phys. Org. Chem.* **2003**, *16*, 450.
(13) Sasamori, T.; Mieda, E.; Nagahora, N.; Takeda, N.; Takagi, N.; Nagase, S.; Tokitoh, N. *Chem. Lett.* **2005**, *34*, 166.
(14) The electron deformation density map of Mes*P═PMes* experimentally observed and the supporting DFT calculations indicated that the HOMO and HOMO-1 of Mes*P═PMes* should be the $n_+$ and $\pi$ orbital, respectively; see: Cowley, A. H.; Decken, A.; Norman, N. C.; Kruger, C.; Lutz, F.; Jacobsen, H.; Ziegler, T. *J. Am. Chem. Soc.* **1997**, *119*, 3389.
(15) Miqueu, K.; Sotiropoulos, J. M.; Pfister-Guillouza, G.; Ranaivonjatovo, H.; Escudié, J. *J. Mol. Struct.* **2001**, *595*, 139.

***Table 1.*** Optimized Structural Parameters[a] for RE═ER Systems[b] and Their Anion Radicals and Kohn−Sham HOMO and LUMO Levels (in eV) of the Neutral Dipnictenes Calculated at B3LYP or UB3LYP/6-31G(d) for C,H:ECP[TZ(2d)+Diffuse] for P, As, Sb, and Bi Levels

| RE═ER | E═P | E═As | E═Sb | E═Bi |
|---|---|---|---|---|
| | | R = H | | |
| KS-LUMO[c] | −3.12 | −3.23 | −3.30 | −3.14 |
| KS-HOMO[c] | −7.30[e] | −7.01[f] | −6.28[f] | −5.91[f] |
| n$D_{E-E}$/Å[c] | 2.046 | 2.268 | 2.653 | 2.765 |
| n∠$_{E-E-R}$/°[c] | 94.4 | 92.6 | 91.2 | 90.3 |
| a$D_{E-E}$/Å[d] | 2.170 | 2.401 | 2.789 | 2.910 |
| a∠$_{E-E-R}$/°[d] | 94.4 | 92.9 | 91.9 | 91.4 |
| | | R = Me | | |
| KS-LUMO[c] | −2.37 | −2.59 | −2.80 | −2.69 |
| KS-HOMO[c] | −6.57[e] | −6.33[f] | −5.77[f] | −5.45[f] |
| n$D_{E-E}$/Å[c] | 2.043 | 2.265 | 2.654 | 2.767 |
| n∠$_{E-E-R}$/°[c] | 101.4 | 99.3 | 97.4 | 96.6 |
| a$D_{E-E}$/Å[d] | 2.153 | 2.389 | 2.786 | 2.910 |
| a∠$_{E-E-R}$/°[d] | 98.7 | 97.0 | 95.6 | 95.0 |
| | | R = Ph | | |
| KS-LUMO[c] | −2.61 | −2.76 | −2.91 | −2.83 |
| KS-HOMO[c] | −5.95[f] | −5.84[f] | −5.59[f] | −5.38[f] |
| n$D_{E-E}$/Å[c] | 2.059 | 2.280 | 2.664 | 2.775 |
| n∠$_{E-E-R}$/°[c] | 101.9 | 99.5 | 97.1 | 95.6 |
| a$D_{E-E}$/Å[d] | 2.152 | 2.390 | 2.786 | 2.907 |
| a∠$_{E-E-R}$/°[d] | 102.2 | 99.6 | 96.8 | 95.6 |
| | | R = Mes | | |
| KS-LUMO[c] | −2.41 | −2.60 | −2.74 | −2.66 |
| KS-HOMO[c] | −5.78[e] | −5.75[e] | −5.62[f] | −5.34[f] |
| n$D_{E-E}$/Å[c] | 2.050 | 2.272 | 2.659 | 2.771 |
| n∠$_{E-E-R}$/°[c] | 101.0 | 99.0 | 97.0 | 95.6 |
| a$D_{E-E}$/Å[d] | 2.170 | 2.402 | 2.789 | 2.908 |
| a∠$_{E-E-R}$/°[d] | 98.5 | 96.4 | 94.4 | 93.3 |

[a] $D_{E-E}$: E−E bond length. ∠$_{E-R-R}$: E−E−R bond angle. [b] E = P, As, Sb, Bi. R = H, Me, Ph, Mes. [c] Calculated for neutral species of RE═ER. [d] Calculated for anion radical species, [REER]•−. [e] $n_+$ orbital. [f] $\pi$ orbital.

tions on dipnictenes using model compounds, RE═ER (E = P, As, Sb, Bi), having less bulky substituents such as H, Me, Ph, and Mes (mesityl). The structural parameters of the model compounds of less hindered dipnictenes optimized at the level of B3LYP/6-31G(d) for C, H, and ECP[TZ(2d)+diffuse] for P, As, Sb, and Bi are in good agreement with those experimentally obtained by the X-ray crystallographic analysis of BbtE═EBbt.[9,10,12] Meanwhile, redox behaviors observed in cyclic voltammetry are not "vertical" but "adiabatic" electron transitions because there is enough time for geometry relaxation during the redox process of cyclic voltammetry. Therefore, we calculated the adiabatic electron affinity (EA), which represents the difference between the total energies of the neutral and anionic species [EA = $E$([REER]) − $E$([REER]•−)] of RE═ER systems (E = P, As, Sb, and Bi; R = H, Me, Ph, and Mes).[16]

The optimized geometries of $[R_2E_2]^{\bullet-}$ (E = P, As, Sb, Bi; R = H, Me, Ph, Mes) are similar to those of the corresponding neutral species except for the slightly longer E−E bond lengths (Table 1), supporting that the SOMOs are simple $\pi$* orbitals of the E═E double bonds (Figure 2). In all cases of R = H, Me, Ph, and Mes, the calculated EAs of RE═ER were found to increase on going from P to Sb, but the EAs of dibismuthenes decreased as compared with those of distibenes (Figure 3). That

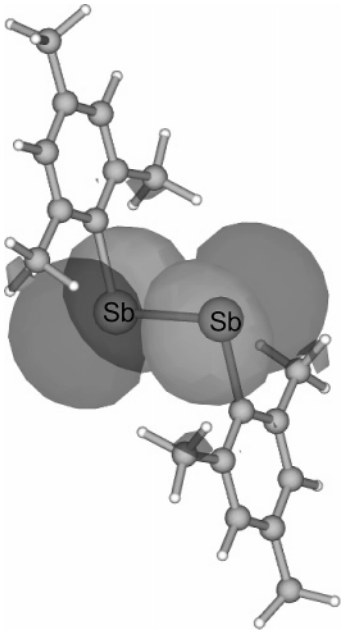


***Figure 2.*** SOMO orbital of [MesSb═SbMes]•− calculated at UB3LYP/6-31G(d) for C,H:ECP[TZ(2d)+diffuse] for the Sb level.

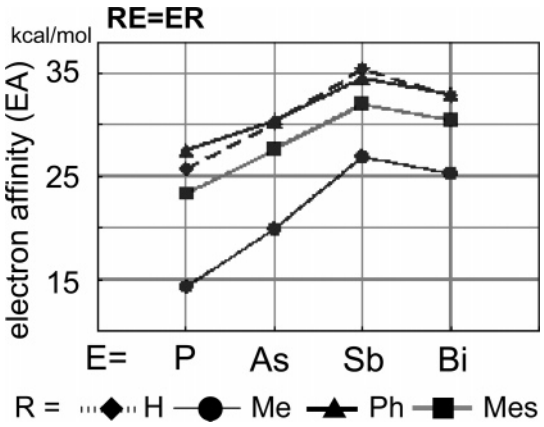


***Figure 3.*** Calculated electron affinities for RE═ER (E = P, As, Sb, Bi; R = H, Me, Ph, Mes) at B3LYP or UB3LYP/6-31G(d) for C,H:ECP[TZ(2d)+diffuse] for the P, As, Sb, and Bi levels.

is, the calculations indicate that the one-electron reduction of RSb═SbR systems is the most exothermic reaction among those of diphosphenes, diarsenes, and dibismuthenes. Thus, this theoretical interpretation is consistent with the experimental results observed in cyclic voltammetry. It is useful to think of the tendencies of EA values in analogy to their LUMO levels, which mainly consist of $\pi$* orbitals of E═E double bonds (Table 1). The same tendency was found in the calculations of their Kohn−Sham (KS) LUMO levels; that is, distibene systems have the lowest KS-LUMO levels in the calculations, supporting the experimental results and calculations of their EAs.

The unique tendency of $\pi$ electron systems of heavier group 15 elements observed here is contradictory to the intuitive expectation that the $\pi$* orbital level of an E═E double bond will be lowered as the element row descends. It can be most likely interpreted in terms of the "relativistic effect of the sixth row elements".[17] It may be expected that the sizes of the valence

(16) B3LYP was selected as a calculation method because the EA values calculated by the DFT method for several examples of atoms and molecules containing heavier main group elements are known to be in excellent agreement with the corresponding experimental data; see: Rienstra-Kiracofe, J. C.; Tschumper, G. S.; Schaefer, H. F.; Nandi, S.; Ellison, G. B. *Chem. Rev.* **2002**, *102*, 231.

(17) (a) Nagase, S. In *The Chemistry of Organic Arsenic, Antimony and Bismuth compounds*; Patai, S., Ed.; Wiley: New York, 1994; Chapter 1, p 1. (b) Pyykkö, P. *Chem. Rev.* **1988**, *88*, 563.

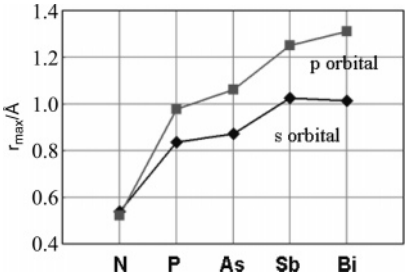


***Figure 4.*** Sizes of valence *n*s and *n*p orbitals of group 15 atoms.

*n*s and *n*p orbitals increase monotonically on going down the periodic table from N to Bi together with the increase of the principal quantum number (*n*). However, the 6s orbital of Bi is known to shrink to nearly the same size as the 5s orbital of Sb due to "relativistic effects" (Figure 4).[17] The shrinkage of 6s may give rise to the unexpectedly smaller difference between the Bi═Bi bond lengths in ArBi═BiAr (Ar = bulky aryl substituent)[9,11] and the Sb═Sb bond lengths in ArSb═SbAr[9,11] (ca. 0.2 Å) than that between the Sb═Sb bond lengths in ArSb═SbAr and the As═As bond lengths in ArAs═AsAr[11] (ca. 0.4 Å) probably due to the smaller antibonding interaction between 6s−6s orbitals in the Bi═Bi double bond. Calculated structural parameters for the RE═ER systems (R = H, Me, Ph, and Mes) also supported such a tendency for bond lengths (Table 1). Consequently, it can be concluded as follows. Stable $\pi$ bonds should be constructed by favorable overlapping of p orbitals. Essential factors for effective overlapping of p orbitals of the E═E bond should be caused by (A) shorter bond lengths and (B) larger p orbitals. In the case of P, As, and Sb, the order of the overlapping of p orbitals, which indicates the strengths of the $\pi$ bonds, is P═P > As═As > Sb═Sb because the factor of (A) is much more effective than (B). On the other hand, the bond length of a Bi═Bi bond is longer than that of an Sb═Sb bond by only ca. 0.2 Å due to the relativistic effect as described above. Therefore, the overlapping of 6p orbitals in dibismuthene is not so unfavorable compared with the case of 5p orbitals in distibene. On the contrary to the shrinkage of 6s orbitals, the size of 6p orbitals is larger than that of the 5p orbital because p orbitals are not so affected by the relativistic effect.[17] Therefore, the unfavorable factor of (A) should be almost canceled by the favorable factor of (B) in the case of a Bi═Bi bond as compared with an Sb═Sb bond. That is, the energy gap between the $\pi$ and $\pi$* orbitals may be nearly the same in the cases of Sb═Sb and Bi═Bi. It was supported by theoretical calculations for the overlap of the valence *n*p orbitals in HE═EH (E = P, As, Sb, and Bi);[18] that is, the integrals of the overlapping of 5p orbitals in HSb═SbH (0.2137) is almost the same as those of 6p orbitals in HBi═BiH (0.2115), and they are smaller than those of HP═PH (0.2513) and HAs═AsH (0.2329).[13] We came to a conclusion that the $\pi$* energy level of a dibismuthene is higher than that of a distibene because the energy levels of 6p is higher than those of 5p as depicted in Figure 5. It should be noted that the experimental results observed here in cyclic voltammetry could be recognized as experimental evidence of the relativistic effect of the sixth row elements.

(18) The integrals of the overlap of the valence p orbitals were calculated at HF/STO-3G for H:ECP(lanl2mb) for E with the optimized structures calculated at B3LYP/6-31G(d) for H:ECP[TZ(2d)+diffuse] for the P, As, Sb, and Bi levels.

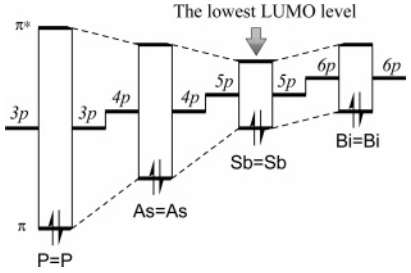


***Figure 5.*** Depiction of the interaction of *n*p orbitals.

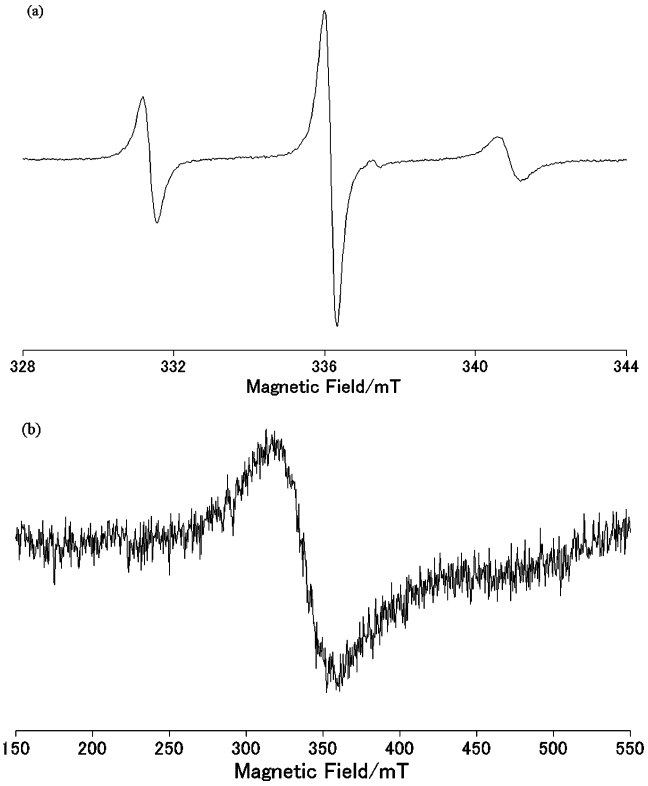


***Figure 6.*** ESR spectrum of (a) **1b**$^{\bullet-}$ and (b) **2b**$^{\bullet-}$ in THF solution.

**Chemical Reduction of Diphosphene 1b, Distibene 2b, and Dibismuthene 3b.** The systematic studies on the redox behavior described above naturally prompted us to obtain the anion radical species of the dipnictenes, **1b**, **2b**, and **3b**. Although there are a number of reports on the ESR observation of anion radical species of kinetically stabilized dipnictenes (diphosphene, diarsenes, and phospharsenes) generated in situ,[5,7] such radical species cannot be in hand as "*bottlable*" crystalline compounds most likely due to their extremely high reactivity and/or instability. Furthermore, there is no report on the attempted generation of the anion radical species of a distibene and a dibismuthene. Such situations prompted us to examine the chemical reduction of the kinetically stabilized dipnictenes, BbtE═EBbt (E = P, Sb, and Bi), leading to the formation of stable anion radical species.

The reduction of diphosphene **1b** with lithium metal in DME afforded a purple solution. The formation of the anion radical species of **1b** was confirmed by the ESR spectrum (Figure 6a), which displayed a hyperfine structure due to 2 equiv of phosphorus atoms [$g$ = 2.009, $a$($^{31}$P) = 135 MHz] as well as the previously reported anion radical species of kinetically stabilized diphosphenes [$g$ = 2.007−2.018, $a$($^{31}$P) = 120−150 MHz].[6] The lithium salt of **1b**$^{\bullet-}$ was successfully isolated as a

***Scheme 2***

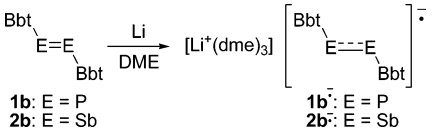


stable purple powder of $[Li^+(dme)_3][\mathbf{1b}^{\bullet-}]$ in 53% yield by the removal of the solvent from the supernatant of the reaction mixture followed by washing with hexane.[19]

Distibene **2b** could also be reduced with lithium metal to give the corresponding anion radical species (Scheme 2). The color of **2b** in DME changed from orange to dark brown after the reduction. Purification procedures similar to the case of $[Li^+(dme)_3][\mathbf{1b}^{\bullet-}]$ afforded $[Li^+(dme)_3][\mathbf{2b}^{\bullet-}]$[19] (53%) as a stable, brown-colored crystalline compound.

The THF solution of $[Li^+(dme)_3][\mathbf{2b}^{\bullet-}]$ showed a highly broadened signal with $g = 2.097$ in the X-band ESR spectrum (Figure 6b). The $g$ value of $\mathbf{2b}^{\bullet-}$ is consistent with an isotropic term of the $g$ tensor ($g^{iso} = 2.1197$) obtained from the following powder-pattern ESR spectra. The powder of the isolated anion radical species was certainly ESR active, and a complicated spectrum showed up (Figure 7). The complexity of the observed spectrum, which is most likely interpreted in terms of the natural abundance of two isotopes of antimony, $^{121}$Sb (57.25%, $I = 5/2$) and $^{123}$Sb (42.75%, $I = 7/2$), made it seemingly difficult to estimate the hyperfine structures and the $g$ values.[20] In this work, the $g$ values and $^{121}$Sb-hyperfine anisotropic coupling constants can be estimated as $g_{xx} = 1.961$, $g_{yy} = 2.030$, $g_{zz} = 2.368$, $A_{xx} = 644$ MHz, $A_{yy} = 350$ MHz, and $A_{zz} = 126$ MHz on the basis of the simulation of the X- and Q-band ESR spectra in the solid state by EasySpin 2.2.0.[21] It should be noted that the complicated spectra can be reasonably explained by the coupling with two antimony atoms, indicating that the bulkiness of the Bbt groups of $\mathbf{2b}^{\bullet-}$ might prevent the intermolecular interaction of the radical species.

The $^7$Li NMR spectra of the THF solutions of the lithium salts of $\mathbf{1b}^{\bullet-}$ and $\mathbf{2b}^{\bullet-}$ showed singlet signals at $-0.02$ and $-0.30$ ppm, respectively, indicating less interaction between the Li cations and the anion radical species in the THF solution probably due to the steric reason. The UV−vis spectra of the anion radicals $\mathbf{1b}^{\bullet-}$ and $\mathbf{2b}^{\bullet-}$ in DME showed characteristic absorption maxima in the region of longer wavelengths at 539 ($\epsilon$ 6000) nm for $\mathbf{1b}^{\bullet-}$ and 812 ($\epsilon$ 2800) nm for $\mathbf{2b}^{\bullet-}$. These absorptions can be assigned to the corresponding $\pi-\pi^*$ electron transitions on the basis of the comparison with the results of TDDFT calculations on the model compounds, $[Mes_2P_2]^{\bullet-}$ and

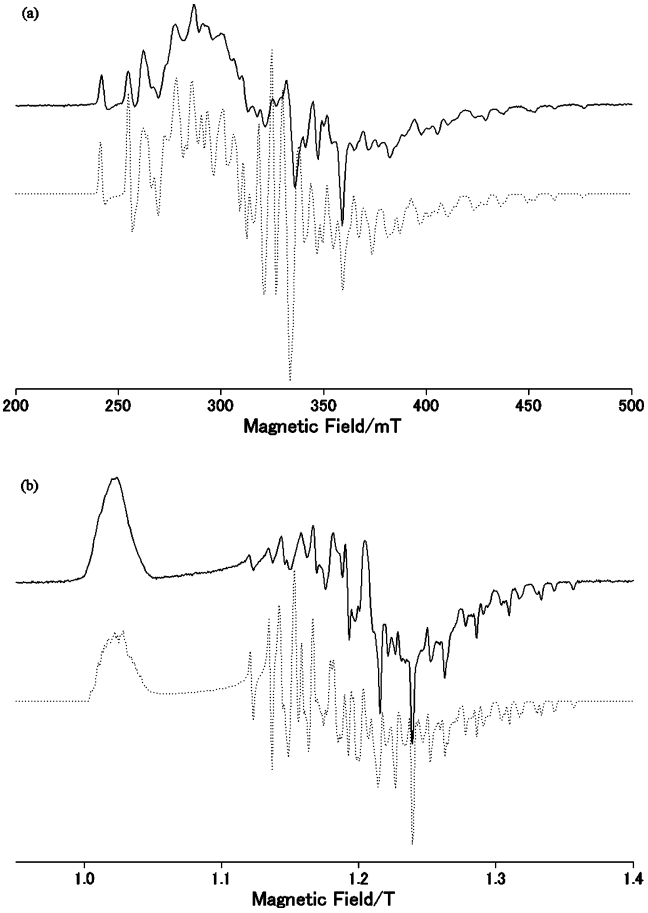


***Figure 7.*** (a) X- and (b) Q-band ESR spectra of $[Li^+(dme)_3][\mathbf{2b}^{\bullet-}]$ in the solid state [upper (observed); bottom (simulated)].

$[Mes_2Sb_2]^{\bullet-}$ (Mes = mesityl), the $\pi-\pi^*$ transitions of which are estimated as 479 and 728 nm, respectively.[22] Thus, the $\pi-\pi^*$ transitions of $\mathbf{1b}^{\bullet-}$ and $\mathbf{2b}^{\bullet-}$ are red shifted as compared with those of the corresponding neutral species (**1b**, 418 nm; **2b** 490 nm),[9] indicating their weakened $\pi$-bonds.

The structural parameters of $[Li^+(dme)_3][\mathbf{2b}^{\bullet-}]$ (Figure 8) were definitively determined by X-ray crystallographic analysis, though $[Li^+(dme)_3][\mathbf{1b}^{\bullet-}]$ has not been structurally characterized so far. There should be no interaction between $[\mathbf{2b}^{\bullet-}]$ and $[Li^+(dme)_3]$ moieties in the crystalline state as judged by the long Sb−Li distance (ca. 6.7 Å). The geometry of $[\mathbf{2b}^{\bullet-}]$ is similar to that of **2b**,[9] having a center of symmetry in the middle of its Sb−Sb bond with the trans configuration. The small Sb−Sb−C(Bbt) angle of 102.29(8)° can be explained in terms of the tendency to maintain a $(5s)^2(5p)^3$ configuration of the Sb atoms as well as that observed in **2b** [Sb−Sb−C: 105.38(10)°].[9] The Sb−Sb bond length of $[\mathbf{2b}^{\bullet-}]$ is 2.7511(4) Å, which is the medium value between the Sb−Sb single [2.844(1) Å for $Ph_2Sb-SbPh_2$][23] and double [2.7037(6) Å for BbtSb=SbBbt][8] bonds. The structural parameters obtained here are consistent with those calculated for the model compound, $[Mes_2Sb_2]^{\bullet-}$, indicating that the effect of the countercation ($Li^+$) is certainly

(19) The $^1$H NMR spectral study showed that the three DME molecules should coordinate on the $Li^+$ in the powder obtained here. The purity of the obtained powder of $[Li^+(dme)_3][\mathbf{1b}^{\bullet-}]$ and $[Li^+(dme)_3][\mathbf{2b}^{\bullet-}]$ could not be confirmed by the analytical data because it should be difficult to obtain satisfactory elemental analyses for the anion radical species obtained here due to their incombustibility in the procedure. However, we believe that the obtained compounds should be obtained as an almost pure form on the basis of the highly broadened $^1$H NMR spectra except for the signals for the DME molecules. In the case of $[Li^+(dme)_3][\mathbf{2b}^{\bullet-}]$, it should be satisfactorily isolated because a number of single crystals suitable for X-ray crystallographic analysis were obtained.

(20) To our knowledge, there is no paper on the observation of organoantimony radicals by ESR spectroscopy, except for the observation of the radical species of the antimony-containing conjugated systems and the inorganic antimony compounds; See: (a) Colussi, A. J.; Morton, J. R.; Preston, K. F. *J. Phys. Chem.* **1975**, *79*, 1855. (b) Alberti, A.; Hudson, A. *J. Organomet. Chem.* **1979**, *182*, C49. Therefore, no straightforwardly helpful information could be obtained for the detailed analysis of the ESR spectra observed in this work.

(21) Stoll, S.; Schweiger, A. *J. Magn. Reson.* **2005**, *177*, 390.

(22) TD-UB3LYP/6-31G(d) for C,H:ECP[TZ(2d)+diffuse] for P, Sb, and Bi. The excitation energies of MesE=EMes systems (E = P, Sb, and Bi) were found to be estimated as slightly shorter wavelengths than observed $\lambda_{max}$ for the BbtE=EBbt systems in hexane by the calculations at the same level. See Supporting Information.

(23) (a) Becker, G.; Freudenblum, H.; Witthauer, C. *Z. Anorg. Allg. Chem.* **1982**, *492*, 37. (b) von Deuten, K.; Rehder, D. *Cryst. Struct. Commun.* **1980**, *9*, 167.

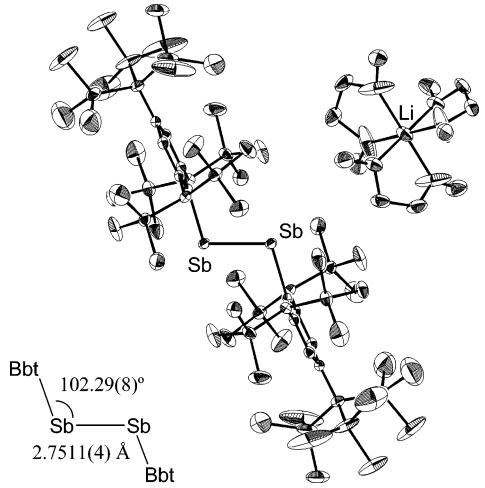


***Figure 8.*** ORTEP drawing of $[Li^+(dme)_3][\mathbf{2b}^{\bullet-}]$ with thermal ellipsoid plots (50% probability).

negligible. On the other hand, the powder of $[Li^+(dme)_3][\mathbf{1b}^{\bullet-}]$ and $[Li^+(dme)_3][\mathbf{2b}^{\bullet-}]$ showed strong Raman lines at 537 and 188 $cm^{-1}$, respectively, which were attributable to the corresponding E−E (E = P and Sb) stretching vibrations. Those of $[Mes_2P_2]^{\bullet-}$ and $[Mes_2Sb_2]^{\bullet-}$ were estimated by the theoretical calculations as 571 and 189 $cm^{-1}$, respectively. The observed E−E stretching frequencies for $[Li^+(dme)_3][\mathbf{1b}^{\bullet-}]$ and $[Li^+(dme)_3][\mathbf{2b}^{\bullet-}]$ are higher than those of the corresponding single bonds (530 $cm^{-1}$ for $Ph_2P-PPh_2$[24] and 141 $cm^{-1}$ for $Ph_2Sb-SbPh_2$[25]) and lower than those of the corresponding double bonds (603 $cm^{-1}$ for BbtP═PBbt[12] and 196 $cm^{-1}$ for BbtSb═SbBbt[9]). These features of the anion radical species $\mathbf{1b}^{\bullet-}$ and $\mathbf{2b}^{\bullet-}$ were reasonably explained in terms of the introduction of one electron onto the antibonding $\pi^*$ orbital of the neutral double bond compounds, **1b** and **2b**, leading to the elongation of the E−E (E = P, Sb) bond lengths. Thus, it was experimentally evidenced that the LUMO of the dipnictenes (**1b** and **2b**) and the SOMO of the anion radical species ($\mathbf{1b}^{\bullet-}$ and $\mathbf{2b}^{\bullet-}$) are the $\pi^*$ orbitals as theoretical calculations predicted.

The reduction of dibismuthene **3b** was performed under the same conditions as those for **1b** and **2b** to give the dark brown solution ($\lambda_{max}$ = 804 nm in the UV−vis spectra), indicating the formation of the corresponding anion radical species, $\mathbf{3b}^{\bullet-}$. The generation of $\mathbf{3b}^{\bullet-}$ was supported by the computed $\lambda_{max}$ value of 805 nm for the $\pi-\pi^*$ electron transition of the model compound, $[MesBi═BiMes]^{\bullet-}$, obtained by the TDDFT calculations.[22] Unfortunately, however, identification and isolation of the products were unsuccessful at present due to its ready decomposition to give the ESR-silent green solution containing BbtH.

## Conclusion

In this paper, we reported the redox behavior of the kinetically stabilized dipnictenes, i.e., diphosphene **1b**, distibene **2b**, and dibismuthene **3b**, using cyclic voltammetry and theoretical calculations. The systematic comparison of the electrochemical properties of dipnictenes led us to demonstrate experimental evidence for the relativistic effect of bismuth. Furthermore, the anion radical species of the diphosphene **1b** and distibene **2b** were successfully synthesized as powder of the lithium salts, which can be in hand as "*bottlable*" powder. The molecular structure of the first stable distibene anion radical, $[Li^+(dme)_3][\mathbf{2b}^{\bullet-}]$, was revealed by X-ray crystallographic analysis. In addition, the UV−vis, ESR, and Raman spectra disclosed the electronic and molecular structures of the radical anions $\mathbf{1b}^{\bullet-}$ and $\mathbf{2b}^{\bullet-}$ in solution and in the solid state. We hope that the unique electrochemical properties of dipnictenes reported here will lead to not only further progress in the main group elements chemistry but also novel application of *heavy dipnictenes* to material science.

## Experimental Section

**General Procedure.** All experiments were performed under an argon atmosphere unless otherwise noted. All solvents were purified by standard methods and/or The Ultimate Solvent System (GlassContour Company)[26] prior to use. Raman spectra were measured on a Raman spectrometer consisting of a Spex 1877 Triplemate and an EG&G PARC 1421 intensified photodiode array detector. An NEC GLG 108 He/Ne laser (632.8 nm for $[Li^+(dme)_3][\mathbf{1b}^{\bullet-}]$, 830 nm for $[Li^+(dme)_3][\mathbf{2b}^{\bullet-}]$) was used for Raman excitation. All melting points were determined on a Yanaco micro-melting-point apparatus and are uncorrected. The electrochemical experiments were carried out with an ALS 600A potentiostat/galvanostat using a glassy carbon disk working electrode, a Pt wire counter electrode, and a Ag/0.01 M $AgNO_3$ reference electrode. The measurements were carried out in $CH_2Cl_2$ and THF solution containing 0.1 M *n*-$Bu_4NBF_4$ as a supporting electrolyte with scan rates of 10−500 mV $s^{-1}$ in a glovebox filled with argon at −50 °C (for oxidation) and room temperature (for reduction). The X-band ESR spectrum of $[Li^+(dme)_3][\mathbf{1b}^{\bullet-}]$ and X- and Q-band ESR spectra of $[Li^+(dme)_3][\mathbf{2b}^{\bullet-}]$ were recorded on Bruker EMX and Bruker E500 spectrometers, respectively. All melting points were determined on a Yanaco micro-melting-point apparatus and are uncorrected. BbtP═PBbt (**1b**), BbtSb═SbBbt (**2b**), and BbtBi═BiBbt (**3b**) were prepared according to the reported procedures.[9,12]

**Synthesis of Diphosphene Anion Radical $[Li^+(dme)_3][\mathbf{1b}^{\bullet-}]$.** To a solution of BbtP═PBbt (**1b**, 52.1 mg, 0.040 mmol) in DME (1 mL) was added a lithium shot (1.0 mg, 0.25 mmol) at room temperature. After 16 h, the color of the reaction mixture turned violet. The residual lithium metal was removed by decantation. The solvent of the resulting solution was evaporated under reduced pressure. The residue was washed with dry hexane several times to give a violet powder of $[Li^+(dme)_3][\mathbf{1b}^{\bullet-}]$ (33.3 mg, 0.022 mmol, 53%). $[Li^+(dme)_3][\mathbf{1b}^{\bullet-}]$: mp 121 °C (decomp).

**Experimental Procedures for the Synthesis of Distibene Anion Radical $[Li^+(dme)_3][\mathbf{2b}^{\bullet-}]$.** To a solution of BbtSb═SbBbt (**2**, 102 mg, 0.069 mmol) in DME (1 mL) was added a lithium shot (1.0 mg, 0.25 mmol) at room temperature. After 4 h, the color of the reaction mixture turned purple. The residual lithium metal was removed by decantation. The solvent of the resulting solution was evaporated under reduced pressure. The residue was washed with dry hexane several times to give a brown powder of $[Li(dme)_3]^+[\mathbf{2b}^{\bullet-}]$ (65.5 mg, 0.037 mmol, 53%). $[Li^+(dme)_3][\mathbf{1b}^{\bullet-}]$: mp 143 °C (decomp).

**ESR Measurements and Analysis of $[Li^+(dme)_3][\mathbf{2b}^{\bullet-}]$.** In solution: An X-band ESR spectrum of $[Li^+(dme)_3][\mathbf{2b}^{\bullet-}]$ observed at room temperature in a THF solution is shown in Figure 6. The following experimental conditions were used: $\nu_{MW}$ = 9.874597 GHz; microwave power, 3.294 mW; modulation frequency, 100 kHz; and modulation amplitude, 0.1 mT.

In the solid state: Multifrequency ESR measurements (X- and Q-band) of $[Li^+(dme)_3][\mathbf{2b}^{\bullet-}]$ were carried out at room temperature using a Bruker E500 spectrometer. A super high Q resonator, ER 4123SHQE, was applied for the X-band measurements. Microwave frequency was calibrated by an Agilent 53152A frequency counter.

(24) Hassler, K.; Hofler, F. *Z. Anorg. Allg. Chem.* **1978**, *443*, 125.
(25) Bürger, H.; Eujen, R.; Becker, G.; Mundt, O.; Westerhausen, M.; Witthauer, C. *J. Mol. Struct.* **1983**, *98*, 265.
(26) Pangborn, A. B.; Giardello, M. A.; Grubbs, R. H.; Rosen, R. K.; Timmers, F. J. *Organometallics* **1996**, *15*, 1518.

Microwave frequencies applied for X- and Q-bands were 9.876331 and 34.03850 GHz, respectively. Spectral simulation of the powder-pattern ESR spectrum was performed by EasySpin 2.2.0, which is a highly generalized Matlab toolbox for ESR spectroscopy. The observed and simulated X- and Q-band ESR spectra of $[Li^+(dme)_3][\mathbf{2b}^{\bullet-}]$ are given in Figures 7a and 7b, respectively.

**X-ray Crystallographic Analysis of $[Li^+(dme)_3][\mathbf{2b}^{\bullet-}]$.** The intensity data were collected on a Rigaku/MSC Mercury CCD diffractometer with graphite monochromated Mo Kα radiation ($\lambda = 0.71070$ Å). Single crystals suitable for X-ray analysis were obtained by slow recrystallization from DME at room temperature. A brown crystal ($0.30 \times 0.20 \times 0.10$ mm$^3$) of $[Li^+(dme)_3][\mathbf{2b}^{\bullet-}]$ was mounted on a glass fiber. The structure was solved by a direct method (SHELXS-97[27,28]) and refined by full-matrix least-squares procedures on $F^2$ for all reflections (SHELXL-97[28]). All hydrogen atoms were placed using AFIX instructions, and all other atoms were refined anisotropically. The $C(SiMe_3)_3$ groups at the para position of the Bbt group were disordered and refined with 76 restraints using ISOR, DFIX, and SIMU instructions, and their occupancies were refined (0.81:0.19). The DME molecules are disordered (1:1). Crystal data: $C_{72}H_{164}LiO_6Sb_2Si_{14}$, $M = 1769.73$, $T = 103$-(2) K, monoclinic, $P2_1/n$ (no.14), $a = 14.8773(2)$ Å, $b = 25.2561(3)$ Å, $c = 14.9110(2)$ Å, $\beta = 116.5601(5)°$, $V = 5011.42(11)$ Å$^3$, $Z = 2$, $D_{calcd} = 1.173$ g cm$^{-3}$, $\mu = 0.747$ mm$^{-1}$, $2\theta_{max} = 51.0$, 51 264 measured reflections, 9298 independent reflections ($R_{int} = 0.0266$), 605 refined parameters, GOF = 1.037, R1 = 0.0415 and wR2 = 0.1018 [$I > 2\sigma$-($I$)], R1 = 0. 0501 and wR2 = 0.1096 [for all data], largest diff. peak and hole 1.167 and −0.963 e·Å$^{-3}$ (around the Sb atom).

**Theoretical Calculations.** All calculations were conducted using the Gaussian 98 series of electronic structure programs.[29] It was confirmed by frequency calculations that the optimized structures have minimum energies. The triple-ζ basis set ([3s3p])[30] augmented by two sets of d polarization functions and diffuse functions[31] for P (d exponents 0.537 and 0.153, sp exponents 0.0298), As (d exponents 0.434 and 0.129, sp exponents 0.0262), Sb (d exponents 0.277 and 0.088, sp exponents 0.0219), and Bi (d exponents 0.229 and 0.069, sp exponents 0.0204) were used with an effective core potential. The 6-31G(d) basis sets were used for C and H.

**Acknowledgment.** This work was partially supported by Grants-in-Aid for COE Research on "Elements Science" (No. 12CE2005), Creative Scientific Research (17GS0207), Scientific Research on Priority Area (No. 14078213, "Reaction Control of Dynamic Complexes"), Young Scientist (B) (Nos. 16750033 and 18750030), Nanotechnology Support Program, and the 21st Century COE on Kyoto University Alliance for Chemistry from the Ministry of Education, Culture, Sports, Science and Technology, Japan. We are grateful to Dr. Nobuhiro Takeda, Assistant Professor, Institute for Chemical Research, Kyoto University, for the fruitful discussions. T.S. thanks Kinki Invention Center for the research grant.

**Supporting Information Available:** X-ray crystallographic data of $[Li^+(dme)_3][\mathbf{2b}^{\bullet-}]$ in a CIF format. Complete ref 29 and the optimized coordinates of the model compounds in PDF format. This material is available free of charge via the Internet at http://pubs.acs.org.

JA064062M

(27) Sheldrick, G. M. *Acta Crystallogr. Sect. A* **1990**, *46*, 467.
(28) Sheldrick, G. *SHELX-97 Program for Crystal Structure Solution and the Refinement of Crystal Structures*; Institüt für Anorganische Chemie der Universität Göttingen: Tammanstrasse 4, D-3400 Göttingen, Germany, 1997.
(29) Frisch, M. J. et al. *Gaussian 98*; Gaussian, Inc.: Pittsburgh, PA, 1998.
(30) Wadt, W. R.; Hay, P. J. *J. Chem. Phys.* **1985**, *82*, 284.
(31) Check, C. E.; Faust, T. O.; Bailey, J. M.; Wright, B. J.; Gilbert, T. M.; Sunderlin, L. S. *J. Phys. Chem. A* **2001**, *105*, 8111.